Polymer 49 (2008) 5482–5489

Contents lists available at ScienceDirect

Polymer

journal homepage: www.elsevier.com/locate/polymer

New copper(II) complexes of polyampholyte and polyelectrolyte polymers: Solid-state NMR, FTIR, XRPD and thermal analyses

Juan Manuel Lázaro Martínez [a], Ana Karina Chattah [b,*], Gustavo Alberto Monti [b], María Florencia Leal Denis [c], Graciela Yolanda Buldain [a], Viviana Campo Dall' Orto [c,**]

[a] Departamento de Química Orgánica, Facultad de Farmacia y Bioquímica, Universidad de Buenos Aires, Junín 956 (C1113AAD), Ciudad Autónoma de Buenos Aires, Argentina
[b] Facultad de Matemática, Astronomía y Física, Universidad Nacional de Córdoba, IFFAMAF-CONICET, 5000 Córdoba, Argentina
[c] Departamento de Química Analítica y Fisicoquímica, Facultad de Farmacia y Bioquímica, Universidad de Buenos Aires, Junín 956 (C1113AAD), Ciudad Autónoma de Buenos Aires, Argentina

ARTICLE INFO

Article history:
Received 4 June 2008
Received in revised form
23 September 2008
Accepted 3 October 2008
Available online 21 October 2008

Keywords:
Copper complexes
Solid-state NMR
Molecular dynamics

ABSTRACT

Novel solid copper(II) complexes were obtained from the polyampholyte poly(EGDE–MAA–IM) and the polyelectrolyte poly(EGDE–MAA) polymers with copper salts at different concentration levels.
The materials were characterized employing solid-state Nuclear Magnetic Resonance (NMR), Fourier Transform infrared (FTIR), X-ray powder diffraction (XRPD), differential scanning calorimetry (DSC) and thermogravimetry (TG).
The reticulation induced by MAA in these materials against the poly(EGDE–IM) gel was analyzed by DSC. The coordination behavior of the carboxylic acid of MAA, compared to that provided by the imidazole ring, was studied through solid-state ^{13}C NMR and changes in the FTIR spectra. The non-homogenous character of the doped and undoped materials was analyzed by the glass transition temperature (T_g), 2D ^{1}H–^{13}C WISE NMR and proton spin–lattice relaxation time in the rotating frame ($T^{H}_{1\rho}$). In particular, the $T^{H}_{1\rho}$ and T^{H}_{1} values in the complexes decreased with the Cu(II) concentration, showing the high sensitivity of both parameters to the presence of a paramagnetic ion. Finally, the thermogravimetric studies indicated that the presence of the imidazole ring was decisive for the stability of the Cu(II) complexes and for the undoped polymers.

1. Introduction

Two particular interesting groups of functionalized polymeric materials are the polyampholytes and polyelectrolytes, which combine anionic and cationic groups or one of these on the pendent side chains of different monomer units, respectively [1–4].

These polymeric zwitterions have been used for catalytic reactions such as hydrolysis of organophosphates [5] and for unimolecular decarboxylation [6]. In the same way, polyampholyte–metal complexes have been proved to exhibit catalase-like activity in hydrogen peroxide decomposition [7], selective oxidation of organic substrates with hydrogen peroxide [8], and hydrogenation of ketones [9] among other examples.

We have recently synthesized and reported new non-soluble and non-porous polymeric materials with the characteristics of polyampholyte or polyelectrolyte [10]. The synthetic process involves the opening of the epoxy groups, present in ethylene glycol diglycidyl ether (EGDE), by the action of methacrylic acid (MAA) and a radical polymerization of MAA segments incorporated in the EGDE molecule to give a polyelectrolyte denominated poly-(EGDE–MAA). A polyampholyte is obtained when imidazole (IM) is added to the mixture reaction. In this case, the opening of the epoxy group is carried out by the action of the carboxylic acid of the MAA and the pyridine-type nitrogen of the IM in order to obtain a polymer bearing acid and basic group denominated poly(EGDE–MAA–IM).

The presence of the imidazole ring in this polyampholytes allows us to increase the uptake of copper ion 67 times [10] and the bovine serum albumin adsorption 730 times against the polyelectrolyte [11]. Remarkably, the new complex Cu(II)–polyampholyte acts as an efficient heterogeneous catalyst for H_2O_2 activation and the degradation of methyl orange, an azo dye [12]. The complex combined effectiveness in dye decolorization and ease of recovery. The efficiency of the catalyst was increased with the amount of immobilized Cu(II). Combining an adequate ratio of mass of complex to solution volume with 25 mM $[H_2O_2]_0$, an almost complete removal of the

* Corresponding author. Tel./fax: +54 351 4334051.
** Corresponding author. Tel./fax: +54 11 49648263.
E-mail addresses: chattah@famaf.unc.edu.ar (A.K. Chattah), vcdall@ffyb.uba.ar (V. Campo Dall' Orto).

0032-3861/$ – see front matter © 2008 Elsevier Ltd. All rights reserved.
doi:10.1016/j.polymer.2008.10.011

color was achieved between 10 and 20 min, in a neutral medium at room temperature with a minimal extension of adsorption to the catalytic surface.

This material offers the versatility to complex different metal ions due to the presence of the imidazole ligand and of carboxylate groups in the structure. In Cu(II)–poly(EGDE–MAA–IM) and Cu(II)–poly(EGDE–MAA–2MI) complexes, the imidazole ring has been found to be the main group involved in metal ion uptake and the carboxylic group appears to have a coordinating role only at high concentrations of the metal ion [10]. A similar behavior has been reported for the complexation of copolymers from unsaturated carboxylic acids and vinylimidazole with Cu(II) [13], and for the coordination of Cu(II) to some peptides [14,15].

The aim of the present work was to determine the effects of copper ion at different concentrations, in the poly(EGDE–MAA) and poly(EGDE–MAA–IM) by solid-state NMR, FTIR, XRPD and thermal studies: differential scanning calorimetry (DSC) and thermogravimetric analysis (TGA).

2. Experimental section

2.1. Materials and methods

Poly(EGDE–MAA–IM), poly(EGDE–MAA) and poly(EGDE–IM) were synthesized according to previous reports [10]. Cu(II)–poly(EGDE–MAA–IM) was prepared with 0.100 g of polyampholyte and 2.0 mL of $CuSO_4$ solution in deionized water in concentration levels from 4 to 100 mM. Cu(II)–poly(EGDE–MAA) was prepared with 0.100 g of polyelectrolyte and 2.0 mL of $CuSO_4$ 100 mM solution in deionized water. Then, the samples were centrifuged and filtered after 48 h of contact time. Free Cu(II) concentration in each supernatant solution was able to be determined spectrophotometrically since $Cu(NH_3)_4^{2+}$ (formed by ammonium hydroxide addition) absorbs radiation at 640 nm and allows the determination of the amount of copper per gram of material.

The following abbreviations are used throughout the manuscript:

- A: poly(EGDE–MAA).
- A_1: Cu(II)–poly(EGDE–MAA) with 1 mg of Cu(II) per gram of polymer.
- B: poly(EGDE–MAA–IM).
- B_8: Cu(II)–poly(EGDE–MAA–IM) with 8 mg of Cu(II) per gram of polymer.
- B_{26}: Cu(II)–poly(EGDE–MAA–IM) with 26 mg of Cu(II) per gram of polymer.
- B_{48}: Cu(II)–poly(EGDE–MAA–IM) with 48 mg of Cu(II) per gram of polymer.
- B_{63}: Cu(II)–poly(EGDE–MAA–IM) with 63 mg of Cu(II) per gram of polymer.

Scheme 1 displays the structure of polymers A, B and poly(EGDE–IM) showing the numbering used for assignments of the NMR spectra.

2.2. X-ray powder diffraction (XRPD)

XRPD analysis was carried out with a PW-1390 Philips diffractometer, using nickel-filtered Cu Kα radiation ($\lambda = 1.5378$ nm, 40 kV, 20 mA). A 2θ range from 5 to 80° was investigated using a scanning rate of 60° h^{-1}.

2.3. FTIR

The FTIR spectra of the polymers and their copper complexes were recorded on a Spectrum 1000 Perkin–Elmer spectrometer using KBr pellets. The material was dried and placed in a desiccator at 20 °C prior to pellet preparation.

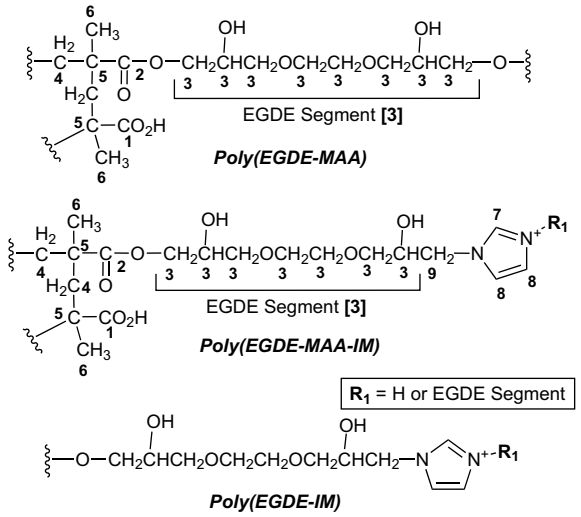

Scheme 1. General chemical structures for polymers A, B and poly(EGDE–IM).

2.4. Differential scanning calorimetry (DSC) and thermogravimetry (TG)

The glass transition temperature (T_g) values of the polymers and their copper complexes were measured on a Shimadzu 60 type differential scanning calorimeter (DSC) at a rate of 15 °C min^{-1} during the second heating trace in the calorimeter under a nitrogen purge. The midpoint of the heat capacity transition between the upper and lower points of the deviation from the extrapolated glass and liquid lines in the DSC curve was taken as the T_g.

Thermogravimetric measurements were carried out with a TA Instrument SDT Q600, under nitrogen flux over a temperature range from 30 to 400 °C with a heating rate of 10 °C min^{-1}. The average sample size was 10 mg.

2.5. Solid-state NMR

High-resolution ^{13}C solid-state spectra for polymer B, polymer A and their copper complexes were recorded using the ramp $\{^1H\} \rightarrow \{^{13}C\}$ CP-MAS (cross-polarization and magic angle spinning) sequence with proton decoupling during acquisition [16]. All the solid-state NMR experiments were performed at room temperature in a Bruker Avance II-300 spectrometer equipped with a 4-mm MAS probe. The operating frequency for protons and carbons was 300.13 and 75.46 MHz, respectively. Adamantane was used as an external reference for the ^{13}C spectra and to set the Hartmann–Hahn matching condition in the cross-polarization experiments. The spinning rate for all the samples was 10 kHz. Different numbers of scans were recorded for each compound in order to obtain an adequate signal to noise ratio. The recycling time was 4 s. The contact time during CP was 800 μs for B_{63} and 1.5 ms for the other compounds. The two-pulse phase modulation (TPPM) sequence was used for heteronuclear decoupling during acquisition with a proton field H_{1H} satisfying $\omega_{1H}/2\pi = \gamma_H H_{1H} = 60$ kHz [17].

Proton spin–lattice relaxation time in the rotating frame, $T^H{}_{1\rho}$, was measured through carbon spectra for polymers A and B and their copper complexes. In this experiment, a cross-polarization sequence is utilized while inserting a proton spin lock during a variable time τ before the contact pulses [16]. During the variable time the rotating frame ^1H spin–lattice relaxation occurs. The experiments were performed at the proton spin-lock field:

$\omega_{1H}/2\pi = 40$ kHz. Additionally, for polymers A, A_1, B and B_{48} the $T^H_{1\rho}$ values were also determined at spin-lock fields of 60 kHz and 83 kHz. The variable time τ was varied from 10 μs to 6 ms. Contact time between carbon and protons was 100 μs, allowing the ^{13}C polarization to be dominated only by the ^1H directly bound to the carbons. Proton spin–lattice relaxation time in the laboratory frame, T^H_1, was measured for A, A_1, B and B_{48}.

The 2D ^1H–^{13}C WISE (wideline separation) experiment was performed following the pulse sequence developed by Schmidt-Rohr et al. for polymers A, A_1, B and B_{48} at room temperature [18]. We selected B_{48} to perform the experiment due to its high concentration of copper ion and good signal to noise ratio compared with B_{63}. In this experiment the initial 90° pulse is followed by an increased time t_1 where the proton magnetization evolves under the influence of dipolar couplings and an isotropic chemical shift. The proton magnetization was transferred to ^{13}C using a short CP contact time of 200 μs in order to avoid equilibration of the proton magnetization due to spin diffusion. The MAS frequency was set to 4.5 kHz in order not to affect the proton lineshape. The 2D WISE experiment correlates structural information in the ^{13}C dimension (chemical shifts) with segmental mobility in the proton dimension (lineshape). In our experiment, 32 increments of 3 μs were collected in the indirect ^1H dimension.

3. Results and discussion

3.1. XRPD analysis

X-ray powder diffraction profiles of the A, A_1, B and B_{63} polymers are depicted in Fig. 1. The lack of sharp peaks in the spectrum of the networks indicates that the polymers are in an amorphous state.

3.2. FTIR studies

Previous ESR reports for the Cu(II)–polyampholyte show that the paramagnetic entities in the solid complex are isolated Cu(II) with a well resolved hyperfine structure in which the copper may be coordinated to the nitrogen of the imidazole and/or the oxygen of the carboxylate with an axial spectrum of a mononuclear square-planar copper(II) species [12].

Fig. 2(a) and (b) shows the FTIR spectra for the A and B polymers and their copper complexes. The complete FTIR analysis of the polymers A and B has been previously reported [10]. The presence of copper produced different spectral changes in the intensity of the signals in the B complexes. Table 1 shows the FTIR assignments for

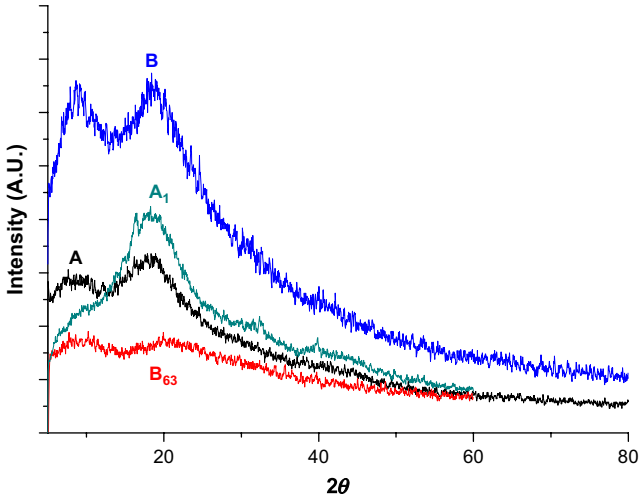

Fig. 1. X-ray powder diffraction profiles for A, A_1, B and B_{63} polymers.

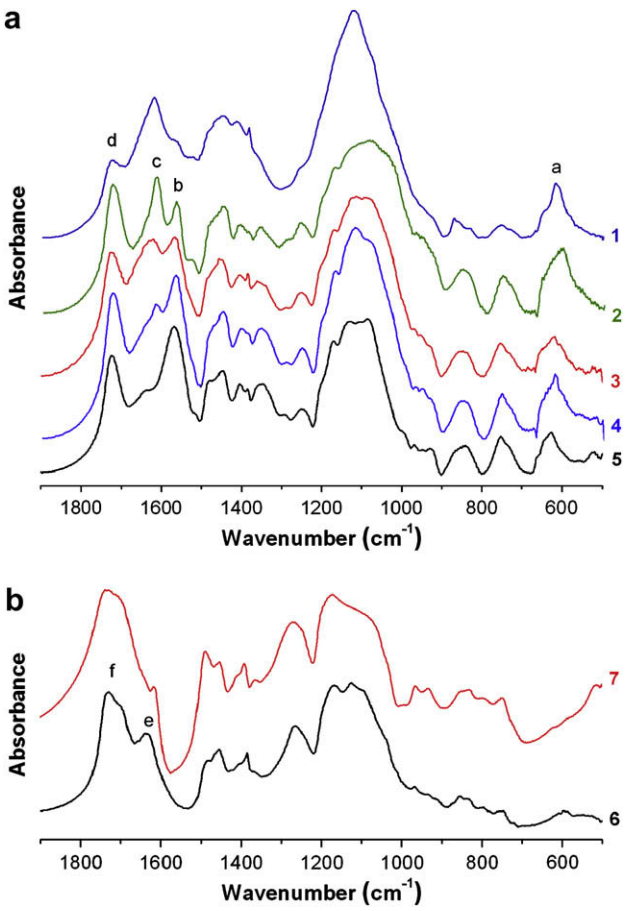

Fig. 2. (a) FTIR spectra for the B_{63} (1), B_{48} (2), B_{26} (3), and B_8 (4) complexes and for the B polymer (5). (b) FTIR spectra for the A (6) and A_1 materials (7).

A, A_1, B and B_{63} materials. The most important spectral changes were: the broadening of the torsion stretching of the imidazole ring at 670 cm^{-1} (Band **a**, Fig. 2(a)), the decrease in the stretching of the carboxylate (υ_{COO^-}) at 1570 cm^{-1} (Band **b**, Fig. 2(a)), and the increase in the stretching of the imidazole ring (υ_{IM}) at 1650 cm^{-1} (Band **c**, Fig. 2(a)) as the copper ion concentration increases. The broadening at 670 cm^{-1} was associated with the overlapping of the torsion stretching of the imidazole ring and the Cu(II)–imidazole complex. The intensity of the υ_{COO^-} can change during different synthetic processes because it depends on the final pH and the ionization degree of the network. The changes produced by the pH or the presence of copper ion have been previously determined [10]. The acidic condition (1 N of HCl solution) produced the disappearance of the υ_{COO^-} and the intensity of the carbonyl

Table 1
FTIR assignments for the A, A_1, B and B_{63} materials.

Stretching vibration (cm^{-1})								
	C=O			C=C/N	CO_2^-	C–O–C	IM[b]	IM–Cu^{II} [b]
	–CO_2R	–CO_2H	–CO_2R/–CO_2H[a]					
A	1740	1730	1705	–	1635	1450–1100	–	–
A_1					–			
B	1722			1650	1570	1450–1100	626–670	–
B_{63}								615

[a] The assignment corresponds to the carbonyl of MAA ester hydrogen bound to the free MAA.
[b] The assignment corresponds to the torsion stretching of the imidazole ring.

stretching ($\upsilon_{C=O}$) at 1730 cm^{-1} (Band **d**, Fig. 2(a)) was higher than the υ_{IM}. However, at 0.1 M of Cu(II) solution, the intensity of the signals was lower for both υ_{COO^-} and $\upsilon_{C=O}$ signals, indicating that these observations were produced by the presence of the copper ion and not by the low acidic medium as given by the coordination process. When the coordination process took place, H^+ from the carboxylic acid (CO_2H) or from the imidazolium ring (IMH^+) was exchanged by a Cu(II), thus lowering the pH of the contact solution to 4.7.

Regarding the A and A_1 materials, we observed that the most significant change was the decrease in the υ_{COO^-} at 1630 cm^{-1} resulting in the coordination with the copper ion (Band **e**, Fig. 2(b)). The **f** band in the spectrum 6 (Fig. 2(b)) was a complex signal because this band was associated with an overlapping of different carbonyl stretchings such as: the $\upsilon_{C=O}$ of the free MAA at 1740 cm^{-1}, the $\upsilon_{C=O}$ of the methacrylic ester at 1730 cm^{-1} and the $\upsilon_{C=O}$ of the MAA ester hydrogen bound to the free MAA at 1705 cm^{-1} [19–21].

Therefore, the υ_{COO^-} disappeared in A and B polymers at 1 and 63 mg of Cu(II) per gram of polymer, respectively. In the B materials, the υ_{COO^-} decreased only at the highest concentration of Cu(II) because the imidazole ring was the main group involved in the copper ion uptake at lower levels, in contrast with A_1, where the only group available for the metal coordination was the carboxylic acid.

3.3. DSC and TG analyses

Fig. 3 shows the DSC curves obtained during the second scan over the temperature range of 20–160 °C and the glass transition temperatures (T_g) for the A, A_1, B and B_{63} polymers. The T_g values are summarized in Table 2 for the materials under study. Fig. 4 shows the DSC curves obtained during the first and the second scan over the temperature range of −30 to 120 °C and the T_g value for the poly(EGDE–IM) gel.

Reticulation is a useful method for improving the properties of a material, including water, solvent and alkali resistance, as well as mechanical strength [22].

The reticulation process increased the glass transition temperature of the B polymer by 34 °C in contrast with the T_g of the poly(EGDE–IM). Additionally, when the MAA monomer was replaced by an equivalent quantity of methyl methacrylate during the synthesis of the A polymer, we found that no reticulation took place between the methyl methacrylic and the EGDE molecule. These results suggest that the reticulation degree in the A and B polymers was caused by the radical polymerization and the opening of the epoxy rings in the EGDE molecule by the action of MAA. Therefore, the non-soluble behavior of the A and B polymers was produced by the high cross-linked degree induced by the MAA monomer, leading the gel character of the poly(EGDE–IM) to become a non-soluble solid material.

Table 2
Glass transition temperatures for A, B and their copper complexes.

Material	T_{g1} (°C)	T_{g2} (°C)	T_{g3} (°C)
A	65.7 ± 0.6	106.9 ± 0.6	–
A_1	65.8 ± 1.0	109.5 ± 0.9	–
B	105 ± 2	–	–
B_8	88 ± 2	131 ± 1	–
B_{26}	84 ± 2	130 ± 1	158 ± 1
B_{48}	92 ± 2	130 ± 1	167 ± 1
B_{63}	117 ± 1	165 ± 1	194 ± 2

The existence of two T_g in the A and A_1 networks was associated with the co-existence of different mobility regions within each polymer. Moreover, the increase in the T_g values for A and B was observed against the poly(EGDE–IM) and a double endothermic transition appeared when MAA was employed in the different combinations. Probably, the MAA polymerization and the incorporation of MAA after the opening of the epoxy group were the main consequences of the co-existence of different mobility regions within the A and B materials.

Two endothermic transitions were observed around 65–70 °C (Point C, Fig. 3) and 95–110 °C in the DSC curve for the B network, but a T_g was possible to determine only in the second one. On the other hand, the effect of the increase in the rigidity of networks with the use of imidazole monomers is well known [23,24]. Then, the presence of the imidazole ring increased the interaction between the different chains and gave more rigidity to the B material, due to the association between the carboxylic acid group with the monosubstituted imidazole ring and the carboxylate group with the disubstituted imidazole ring.

Although the T_{g1} value for the A_1 and A materials was the same in the presence or in the absence of copper, the T_{g2} value for the A_1 complex was slightly shifted to a higher value due to the stabilization of the d-electron of the copper ion [23,25]. Probably, the regions involved in the T_{g2} were associated with the coordination role, in contrast to the non-coordination segments associated with the T_{g1}. The shift in the T_{g2} was not so evident because of the low amount of Cu(II) coordinated in the A_1 complex.

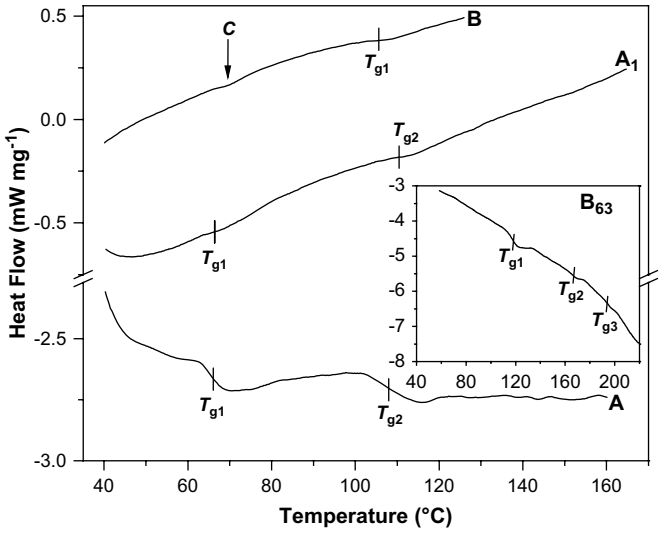

Fig. 3. DSC curves for A, A_1, B and B_{63} materials at the second heating scan.

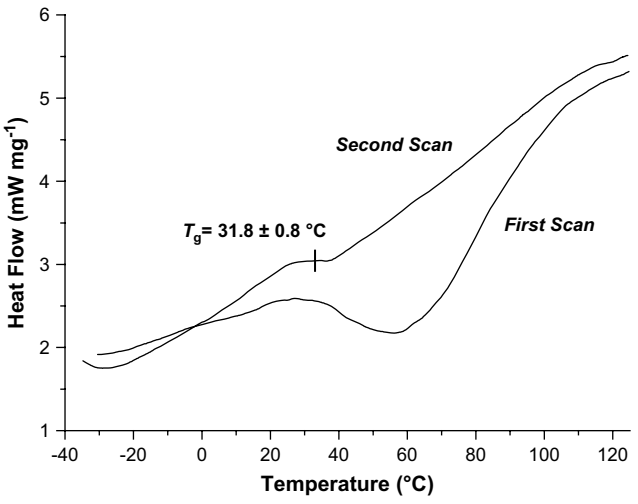

Fig. 4. DSC curves for the poly(EGDE–IM) at the first and second scans.

As it can be seen in Table 2, the B complexes showed new and higher T_g values with the increasing Cu(II) concentration. This behavior was in contrast with previous works where only one T_g is shifted to higher values due to the coordination of different metal ions [25–27]. In our materials the uptake of copper was produced by different ligands within the B polymer as it was observed by FTIR, where MAA became more important for the complexation with the increasing copper ion concentration. These results indicated that the complexation with copper enhanced the intermolecular interaction [27,28].

Figs. 5 and 6 show the TG and DTG curves for the A and B materials, including their Cu(II) complexes, respectively. The thermogravimetric analysis showed an initial loss of weight due to the evaporation of water in all the cases and an endothermic peak in the first DSC scan. The endothermic peak is shown in Fig. 4 for poly(EGDE–IM) as an example and was similar for the rest of the materials at the first heating scan in the DSC experiments. From the comparison of the TG and DTG profiles for the A and B materials, we observed a higher thermal stability in the latter associated with the presence of the imidazole ring in its structure (Figs. 5 and 6). That behavior was observed in copolymers such as poly(*N*-vinylimidazole-*co*-ethylmethacrylate) [29].

All the Cu(II) complexes presented a lower decomposition temperature in contrast with the undoped polymers (A and B). This effect was more intense in the B complexes due to the higher level of copper in the polymer structure (Fig. 6). The presence of the imidazole ring in the backbone increased the coordination properties 67 times if we compared the maximum binding capacity for copper between A and B polymers [10]. Therefore, the presence of the paramagnetic Cu(II) ion center produced changes in the electronic density with the weakness of the chemical bonds and the polymer backbone decreasing its thermal stability.

The decomposition curves of the B_{63} and B_8 complexes were more complex in comparison with B and proceeded in three clear steps (Fig. 6). This could be associated with the different ligands (–CO_2H or –IM group) involved in the coordination of the metal ion, in concordance with the FTIR results [27].

Note that in all the Cu(II) complexes a residual weight was observed due to residual cupric salts after the degradation of the organic matrix.

3.4. Analysis of the ^{13}C NMR spectra

Solid-state NMR is a powerful technique to characterize polymeric compounds. In particular, the high-resolution ^{13}C spectra

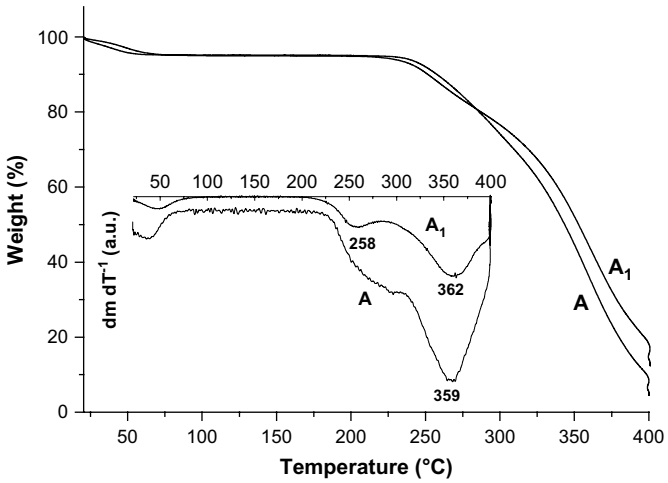

Fig. 5. TG and DTG curves for the A and A_1 materials.

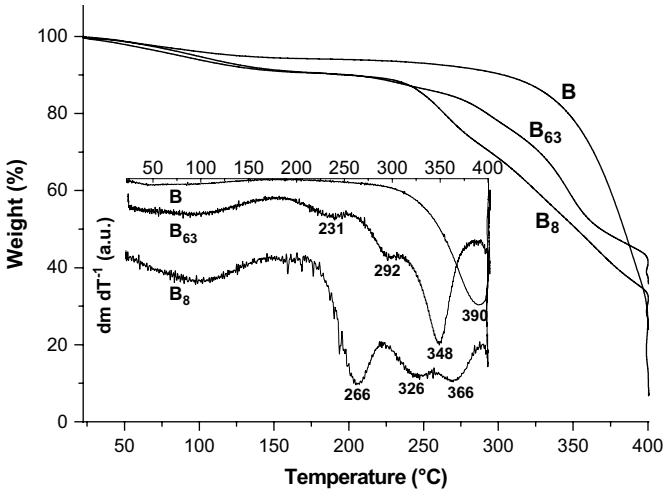

Fig. 6. TG and DTG curves for the B, B_8 and B_{63} materials.

obtained with CP-MAS contain important information on materials that cannot be characterized by diffraction techniques [16]. In addition, this technique has the advantage of retrieving information in a noninvasive way and without the need to modify the samples. Solid-state NMR has been widely used to study polymers and their metal complexes (lithium, copper and iron) [30,31]. The ^{13}C CP-MAS spectra of polymer A and its copper complex A_1 are shown in Fig. 7. Fig. 8 displays the ^{13}C CP-MAS spectra of polymer B and its copper complexes B_8, B_{26}, B_{48} and B_{63}. The numbers of the assignments correspond to those in Scheme 1.

Carbon assignment for polymers A and B has been previously made and is summarized in Table 3 [10]. Fig. 7(a) shows the resonance peaks at 187.2 and 179.4 ppm, which were assigned to the carboxylic acid (C(1)) and the carboxylic ester (C(2)), respectively. The signal at 70.9 ppm corresponds to carbons bound to the ether oxygen (EGDE segment, C(3)). In addition, resonance peaks at 55.3, 45.1 and 16.0 ppm were assigned to the methylene groups (C(4)), quaternary (C(5)) and methyl carbons (C(6)) on the segments of methacrylic acid in the polymer. Fig. 8(a) shows that polymer B also presents the signals of the carbons C(1) and C(2). Carbons of the imidazole ring appeared at 137.8 and 123.7 ppm (C(7) and C(8)), respectively. In addition, there was an overlapping from the signals of methylene carbons of the MAA segments and the EGDE segments bound to the nitrogen of the imidazole ring (carbons denoted by C(9)), which broadens the peak at 53.6 ppm. Note that the signal corresponding to C(9) is absent in polymer A. Both A and B spectra confirm the fact that the materials were amorphous, since the signals have a width at half height that ranges from 160 Hz to 680 Hz.

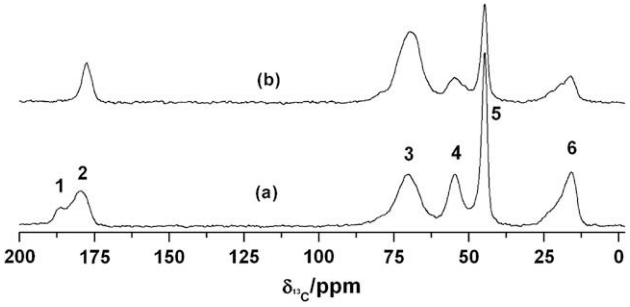

Fig. 7. ^{13}C CP-MAS spectra of polymer A (a) and its copper complex A_1 (b). The numbering corresponds to that in Scheme 1. The number of scans for both spectra was 1600.

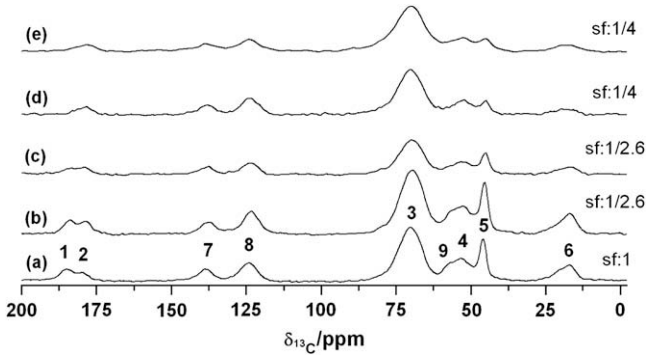

Fig. 8. ^{13}C CP-MAS spectra of: B (a), and the copper complexes B_8 (b), B_{26} (c), B_{48} (d) and B_{63} (e). The labels correspond to those in Scheme 1. The number of scans was: 1000 (a), 2600 in (b) and (c), 4000 in (d) and (e). (Sf: scaling factor).

Comparing the A spectrum with that corresponding to its copper complex A_1 in Fig. 7, we can note the absence of C(1) in the A_1 spectrum, giving evidence that the carboxylic acid was involved in the coordination to copper, in agreement with the FTIR results. The disappearance of this signal was probably due to the dipolar interaction between the ^{13}C and the paramagnetic Cu(II) ion, which provided a strong source of relaxation. In addition, it was possible to see some loss of intensity in signals corresponding to C(4) and C(5), giving support to the evidence that this part of the polymer participated in the bonding to copper.

Comparing the complexes of polymer B it was also possible to see that C(1), C(4) and C(5) were affected by the complexation. In particular, the C(1) signal broadened with the presence of the smaller copper concentrations (B_8 and B_{26}) and was completely reduced in B_{48} and B_{63}. C(4) and C(5) showed decreasing intensities in comparison with the C(3) signal, as the copper concentration increased. It is important to note that the signals corresponding to the imidazole ring were not highly affected by the different copper concentrations, although they participated in the bonding as confirmed by FTIR. This fact marks a difference with the copper complexes of poly(*N*-vinylimidazole-*co*-ethylmethacrylate) (PVM) of reference [23]. In that work the signals corresponding to imidazole carbons are completely reduced in the complex spectrum. The absence of these signals in Cu(II)–PVM50 can be attributed to the fact that all the imidazole rings were available to participate in the coordination to copper at the level concentration assayed (0.16 M of $CuSO_4$). In our case, only 57% of the imidazole rings was available to bind copper, because 43% of the imidazole units are 1,3-disubstituted [10]. Besides, in the B complexes, a competence for the complexation between imidazole and MAA occurred, and then, when the imidazole was saturated, the complexation took place preferentially through MAA, as proved by the absence of C(1) in B_{63} and A_1.

Note that, in general, Figs. 7 and 8 do not show any noticeable shift in the signals of the A and B complexes with respect to those in the spectra of the pure polymers (see also Table 3).

Table 3
^{13}C CP-MAS chemical shifts corresponding to A, A_1, B and B_{63} materials.

δ ^{13}C (ppm)				
A	A_1	B	B_{63}	Assignment[a]
16.0	16.0	17.1	17.7	(**6**)
45.1	44.6	45.8	45.2	(**5**)
55.3	54.9	53.6	52.7	(**4**)
–	–	57.8	–	(**9**)
70.9	69.9	71.3	70.0	(**3**)
–	–	123.7	124.2	(**8**)
–	–	137.8	138.6	(**7**)
179.4	177.6	180.0	178.3	(**2**)
187.2	–	185.0	–	(**1**)

[a] The assignments correspond to those in Scheme 1.

3.5. 2D ^{1}H–^{13}C WISE NMR

2D WISE NMR has been widely used for determining dynamic heterogeneities in solid polymers [18,32,33]. With this technique, the information about the dynamic behavior within the system can be qualitatively assessed by examining the proton line widths associated with the different carbons in the polymer host. The line width of the ^{1}H projections reflects the nature of the dipolar interaction between the protons and can thus be used to monitor the mobility of the polymer chains. Figs. 9 and 10 display the projections on the ^{1}H dimension of the 2D WISE NMR spectra extracted at different ^{13}C chemical shifts for A compared with A_1, and B compared to B_{48}, respectively.

First of all, we can see that the ^{1}H projections associated with C(3) and C(5) in A, and C(3) in B were contributions of two lines with different widths, indicating that the compounds were non-homogeneous, presenting regions with different molecular mobility. These results are in agreement with the DSC data, where two endothermic transitions can be observed for both compounds. The similar values for FWHH (full width at half height displayed in the figures) corresponding to each carbon in A were indicative that there is no *local* (or micro) phase separation in this compound. The same behavior can be observed in B. Then, the representative polymeric chain (MAA–EGDE in A or MAA–EGDE–IM in B) was present in the regions with different mobility. The ^{1}H projection associated with C(6) exhibited the narrowest signal in A and B, due to the fact that this carbon belongs to a CH_3 group that performs rapid rotations, and then averages the dipolar couplings between the three protons. In particular, the ^{1}H projection corresponding to C(8) in B had a smaller width compared to C(3) and C(5); this could be associated with the torsion mobility of the imidazole ring.

Comparing A and B ^{1}H line widths, the FWHHs were smaller in A than the corresponding carbons in B. This result is in agreement with the fact that T_{g1} in B was higher than in A, indicating more mobility in A and that the addition of imidazole gave more rigidity to the main chain.

^{1}H line widths of A_1 were similar to those belonging to A, indicating that the mobility of the different regions in the compound was not strongly changed with the complexation of Cu(II). This is in agreement with the DSC results where the T_{g1}

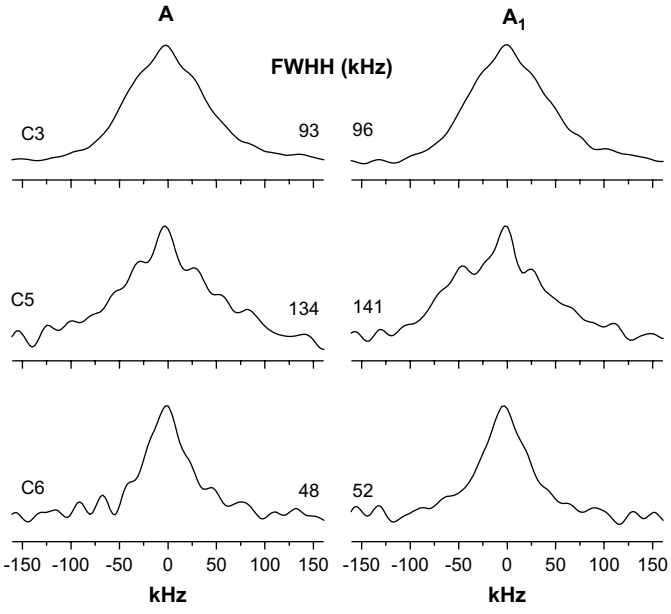

Fig. 9. ^{1}H projection for the corresponding carbons extracted from the 2D WISE experiment in A and A_1. Full width at half height (FWHH) is displayed for each line.

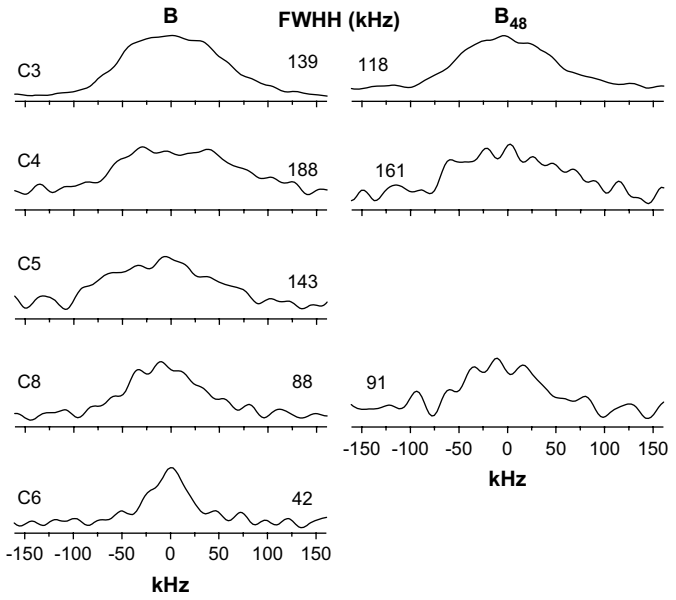

Fig. 10. ^{1}H projection for the corresponding carbons extracted from the 2D WISE experiment in B and B_{48}. The full width at half height (FWHH) is displayed for each line. ^{1}H projections corresponding to C(5) and C(6) in B_{48} are not shown due to the poor signal to noise ratio of these carbons.

values are identical in both compounds and T_{g2} is slightly higher in A_1. The 2D WISE experiment did not reveal consistent differences in the line widths corresponding to B and B_{48} within the experimental error, indicating that the complexation with copper did not significantly affect the structure of the polymer.

3.6. Proton spin–lattice relaxation times: $T^{H}_{1\rho}$ and T^{H}_{1}

Relaxation times in the rotating frame are sensitive to the movements in the kHz scale and can retrieve information on the dynamics in polymeric domains, the homogeneity of the compound and the effect of paramagnetic ions to induce fluctuations in the local magnetic fields [23,32,34–37]. Table 4 displays the $T^{H}_{1\rho}$ values calculated from the carbon signals that were visible in the ^{13}C CP-MAS spectra of polymers A and B and their copper complexes, recorded at 100 μs of contact time and with a spin-lock power of 40 kHz. Figs. 11 and 12 show the semilogarithmic plot of the ^{13}C magnetization as a function of τ, $M_C(\tau)$, for carbons in the EGDE, MAA and IM segments of A and B and their copper complexes.

In general, carbon magnetization in MAA and imidazole segments in all the compounds had a single exponential decay of the form

Table 4
$T^{H}_{1\rho}$ (in ms) measured in A and B and their copper complexes. The values were obtained by fitting the experimental data of ^{13}C magnetization vs. τ to Eq. (1) or (2). Relative errors are within 5%. In the case of the two-exponential decay, the fractions corresponding to the short $T^{H}_{1\rho}$ is displayed in parenthesis. The missing values correspond to cases with poor signal to noise ratio.

Complexes	$T^{H}_{1\rho}$ (EGDE)		$T^{H}_{1\rho}$ (MAA)			$T^{H}_{1\rho}$ (IM)	
	C(3)		C(4)	C(5)	C(6)	C(7)	C(8)
A	3.3	0.5 (37%)	3.4	2.9	3.1	–	–
A_1	2.9	0.42 (33%)	3.2	2.6	2.3	–	–
B	3.3	0.6 (26%)	3.0	2.6	–	2.8	2.8
B_8	1.9	0.3 (33%)	1.7	1.4	–	1.9	1.6
B_{26}	0.9	–	0.9	0.7	–	–	0.8
B_{48}	0.7	–	0.8	–	–	–	0.9
B_{63}	0.5	–	0.5	–	–	–	0.5

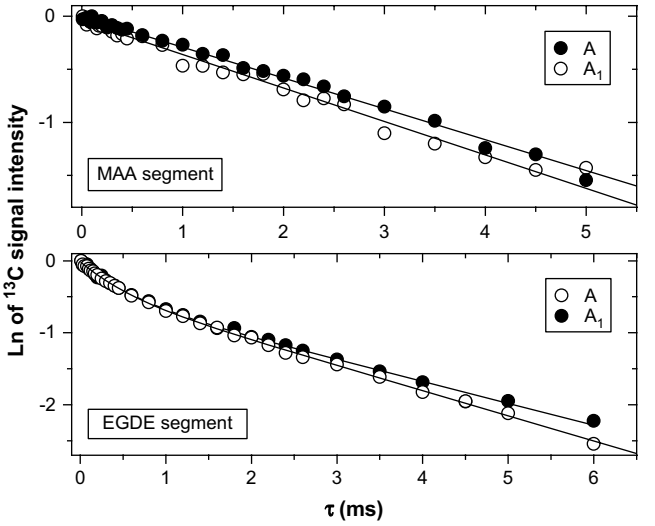

Fig. 11. Semilogarithmic plot of the ^{13}C magnetization as a function of the spin-lock time τ for the $T^{H}_{1\rho}$ experiment in polymer A and its copper complex, A_1. The MAA segment corresponds to the signal at 55.3 ppm while the EGDE segment corresponds to the signal at 70.9 ppm. The fittings of the experimental data to Eqs. (1) and (2) are shown. The fitting values are given in Table 4.

$$M_C(\tau) = M_0 \exp(-\tau/\tau_1) \quad (1)$$

On the other hand, at low copper concentrations, carbon magnetization in the EGDE segment (signal at 70 ppm) followed a two-exponential behavior of the form

$$M_C(\tau) = A \exp(-\tau/\tau_1) + (1 - A)\exp(-\tau/\tau_2) \quad (2)$$

This decay was indicative of a non-homogeneous material having regions with different mobility. Here, as the magnetization had been normalized, the numbers A and (1 – A) can be directly interpreted as a measure of the percentage of the sample giving τ_1 and τ_2, respectively.

The values reported in Table 4 show that the complexation with copper clearly shortens the proton relaxation times in the rotating frame. The relaxation times corresponding to A_1 were slightly

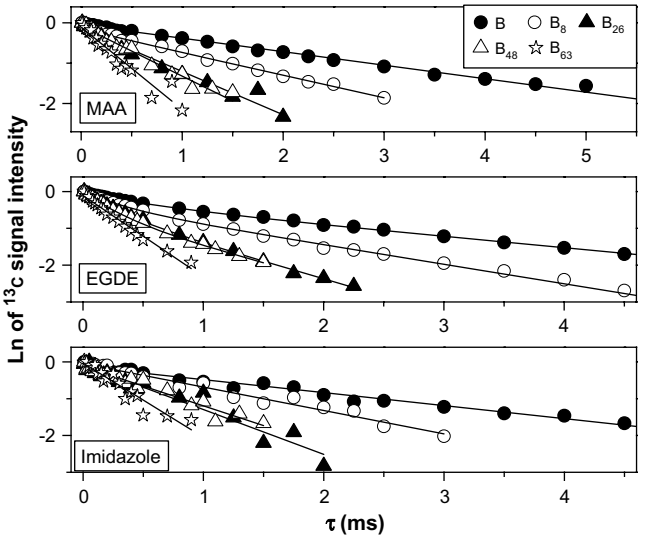

Fig. 12. Semilogarithmic plot of the ^{13}C magnetization as a function of the spin-lock time τ for the $T^{H}_{1\rho}$ experiment in polymer B and its copper complexes. The MAA segment corresponds to the signal at 53.6 ppm, the EGDE segment corresponds to the signal at 71.3 ppm, and the imidazole segment corresponds to the signal at 123.7 ppm. The fittings of the experimental data to Eqs. (1) and (2) are shown. The fitting values are given in Table 4.

shorter than those corresponding to A. In the B complexes the increasing addition of Cu(II) shortened the $T^{H}_{1\rho}$ values, in agreement with results reported in complexes with lithium, copper and ferric ions [23,34,37,38]. From the WISE experiment, we can clearly see that the line widths in the ^{1}H projection for A and A_1 were similar; the same fact can be observed in B compared to B_{48} (Figs. 9 and 10), indicating that there were no changes in mobility with the copper complexation. Then, the decreasing $T^{H}_{1\rho}$ values show that the presence of copper provides a strong source of relaxation [16,32]. In addition, the $T^{H}_{1\rho}$ values measured at 60 kHz and 83 kHz show the same decreasing behavior with the concentration of copper (data not shown). These results indicate that the decrease in the $T^{H}_{1\rho}$ values with the copper ion concentration was not produced by changes in the molecular motions.

On the other hand, Figs. 11 and 12 show a two-exponential decay for the EGDE segment in the case of low copper concentrations, indicating a non-homogeneous material. Fast or effective relaxations (short values for $T^{H}_{1\rho}$) correspond to mobile fractions. These results are in agreement with the DSC data obtained for A, A_1 and B, in which two endothermic transition values were associated with different mobility regions within these polymers. Table 4 also shows that the larger fraction corresponded to a longer relaxation time, indicating more amount of a more rigid phase in these polymers. In particular, the smaller fraction of the more mobile region in B compared with that in A and A_1 could explain the absence of a clear glass transition temperature between 60 and 70 °C in polymer B. The double decay behavior was not observed at high copper concentrations because the $T^{H}_{1\rho}$ decreased dramatically. The EGDE segments presented this two-exponential behavior because this resonance had the best signal to noise ratio in comparison with the other segments.

The proton relaxation time in the laboratory frame, T^{H}_{1}, was measured for A, A_1, B and B_{48}. To complement these experiments in B_{48}, the T^{H}_{1} was also measured through ^{13}C, observing the same behavior for all carbons. The values for A and B were 951 ms and 1600 ms, respectively. In the case of A_1 and B_{48} the values measured were 171 and 7 ms, respectively, showing an important decrease in the relaxation times with the complexation. However, the T^{H}_{1} in the copper complexes presented a non-mono-exponential behavior due to the fact that some polymeric chains are not available for copper ion complexation (10% in A_1 and 1% in B_{48}).

4. Conclusions

New copper(II) complexes of polyampholyte and polyelectrolyte materials have been characterized through different spectroscopic techniques in the solid state. Significant changes in the FTIR and ^{13}C CP-MAS spectra were observed associated with the effects of the copper ions in the polymeric networks.

Notably, it was possible to observe that the carbon signal of the carboxylic acid disappeared in the A and B materials in the ^{13}C CP-MAS spectra at 1 and 63 mg of Cu(II) per gram of material, respectively. In agreement, the FTIR spectra confirmed that the imidazole ring is involved in the copper coordination together with the carboxylic acid.

In the B complexes, a competence for the complexation through imidazole and MAA occurs; then, when the imidazole is saturated, the complexation takes place preferentially through MAA, as concluded from the FTIR and solid-state NMR results.

The amorphicity of the materials was observed by the diffraction profiles obtained.

However, the DSC studies determined the presence of different molecular mobility regions within both A and B polymers, in agreement with the double decay observed in the $T^{H}_{1\rho}$ experiments.

On the other hand, TG analysis gives evidence that the B material bearing the imidazole ring presented a more thermal stability than A, associated with the presence of this ligand. Then, the B complexes have the property of coordinating higher amounts of Cu(II), which explains the lower thermal stability in those materials due to changes in the electronic density in the polymeric matrix. Additionally, the $T^{H}_{1\rho}$ values were sensitive to the presence of copper in the A and B complexes, showing decreasing values with higher concentrations of copper. This fact indicates that copper, as other paramagnetic ions, provides an effective source of fluctuations in the rotating frame, because local magnetic fields are increased. Moreover, the 2D WISE experiments, together with the relaxation experiments (T^{H}_{1} and $T^{H}_{1\rho}$), allow us to conclude that although the relaxation behavior was modified, the paramagnetic ion does not change the structure of the polymer substantially. Additionally, the reticulation increased the T_g in the A and B polymers as a result of the presence of the MAA monomer against poly(EGDE–IM).

Acknowledgements

The authors thank the financial support from Universidad de Buenos Aires (UBACyT 04-07/B005, B037 and B062), CONICET, MinCyT, Secyt-UNC, ANPCyT-FONCyT. Juan Manuel Lázaro Martínez thanks CONICET for his doctoral fellowships.

References

[1] Hadjikallis G, Hadjiyannakou SC, Vamvakaki M, Patrickios CS. Polymer 2002; 43:7269.
[2] Noh JG, Sung YJ, Geckeler KE, Kudaibergenov SE. Polymer 2005;46:2183.
[3] Annenkov VV, Danilovtseva EN, Tenhu H, Aseyev V, Hirvonen SP, Mikhaleva AI. Eur Polym J 2004;40:1027.
[4] Bekturov EA, Kudaibergenov SE, Rafikov SR. Rev Macromol Chem Phys 1990; 30:233.
[5] Bromberg L, Alan Hatton T. Ind Eng Chem Res 2007;46:3296.
[6] Hampton Jr KW, Ford WT. Langmuir 2000;16:7373.
[7] Bekturov EA, Kudaibergenov SE, Sigitov VB. Polymer 1986;27:1269.
[8] Li X, Geng W, Zhou J, Luo W, Wang F, Wang L, et al. New J Chem 2007;31:2088.
[9] Lundgren RJ, Rankin MA, McDonald R, Schatte G, Stradiotto M. Angew Chem Int Ed 2007;46:4732.
[10] Lázaro Martínez JM, Leal Denis MF, Campo Dall' Orto V, Buldain GY. Eur Polym J 2008;44:392.
[11] Leal Denis MF, Carballo RR, Spiaggi AJ, Dabas PC, Campo Dall' Orto V, Lázaro Martínez JM, et al. React Funct Polym 2008;68:169.
[12] Lázaro Martínez JM, Leal Denis MF, Piehl LL, Rubín de Celis E, Buldain GY, Campo Dall' Orto V. Appl Catal B 2008;82:273.
[13] Annenkov VV, Danilotseva EN, Saraev VV, Mikhaleva AI. J Polym Sci Part A Polym Chem 2003;41:2256.
[14] Conato C, Kamysz W, Kozlowski H, Luczkowski M, Mackiewicz Z, Mlynarz P, et al. J Chem Soc Dalton Trans 2002;21:3939.
[15] Kowalik Jankowska T, Ruta Dolejsz M, Wisniewska K, Lankiewicz L. J Inorg Biochem 2001;86:535.
[16] Harris RK. Nuclear magnetic resonance spectroscopy. London: Logman Scientific and Technical; 1994.
[17] Bennett AE, Rienstra CM, Auger M, Lakshmi KV, Griffin RG. J Chem Phys 1995;103:6951.
[18] Schmidt-Rohr K, Clauss J, Spiess HW. Macromolecules 1992;25:3273.
[19] Huang CF, Chang FC. Polymer 2003;44:2965.
[20] Kuo SW, Chang FC. Macromolecules 2001;34:4089.
[21] Motzer HR, Painter PC, Coleman MM. Macromolecules 2001;34:8390.
[22] Chu F, McKenna TF, Jiang Y, Lu S. Polymer 1997;38:6157.
[23] Wu KH, Chang TC, Wang YT, Hong YS, Wu TS. Eur Polym J 2003;39:239.
[24] Chiu YS, Wu KH, Chang TC. Eur Polym J 2003;39:2253.
[25] Belfiore LA, McCurdie MP, Das PK. Polymer 2001;42:9995.
[26] McCurdie MP, Belfiore LA. Polymer 1999;40:2889.
[27] Santana AL, Noda LK, Pires ATN, Bertolino JR. Polym Test 2004;23:839.
[28] Wu KH, Wang YR, Hwu WH. Polym Degrad Stab 2003;79:195.
[29] Pekel N, Şahiner N, Güven O, Rzaev ZMO. Eur Polym J 2001;37:2443.
[30] Köster TKJ, van Wüllen L. Solid State Ionics 2008;178:1879.
[31] Ibbett RN, Domvoglou D, Fasching M. Polymer 2007;48:1287.
[32] Gerbaud G, Hediger S, Gadelle A, Bardet M. Carbohyd Polym 2008;73:64.
[33] Kao HM, Hung TT, Fey GTK. Macromolecules 2007;40:8673.
[34] Hou WH, Chen CY, Wang CC. Solid State Ionics 2004;166:397.
[35] Chattah AK, Garro Linck Y, Monti GA, Levstein PR, Breda SA, Manzo RH, et al. Magn Reson Chem 2007;45:850.
[36] Gabrielse W, Angad Gaur H, Feyen FC, Veeman WS. Macromolecules 1994; 27:5811.
[37] Pfeffer PE, Gerasimowicz WV, Piotrowski EG. Anal Chem 1984;56:734.
[38] Ruhnau FC, Veeman WS. Macromolecules 1996;29:2916.